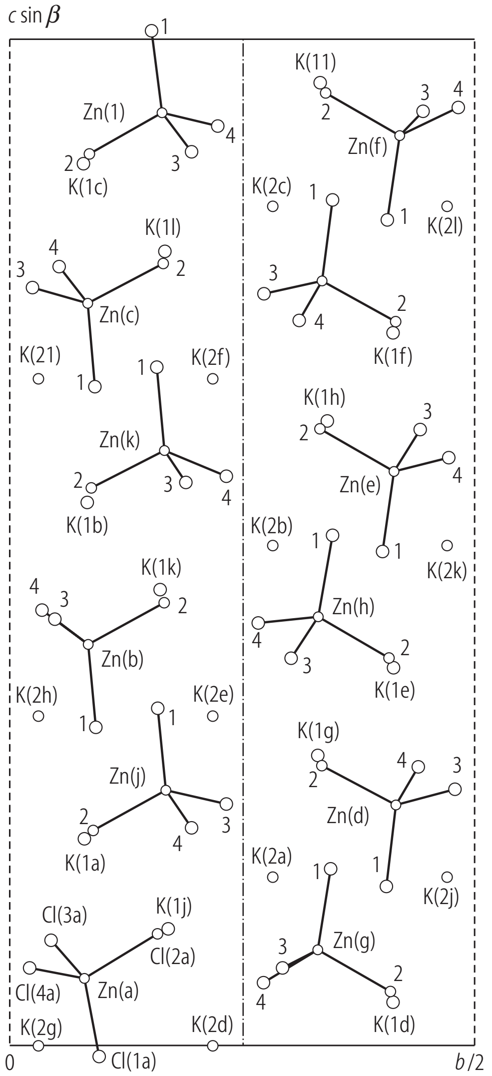

Fig. 39A-9-001. K_2ZnCl_4. Crystal structure of phase IV [93Mas]. Projection along *a* axis. Only independent atoms in one quarter of the unit cell are shown. T = 140 K.

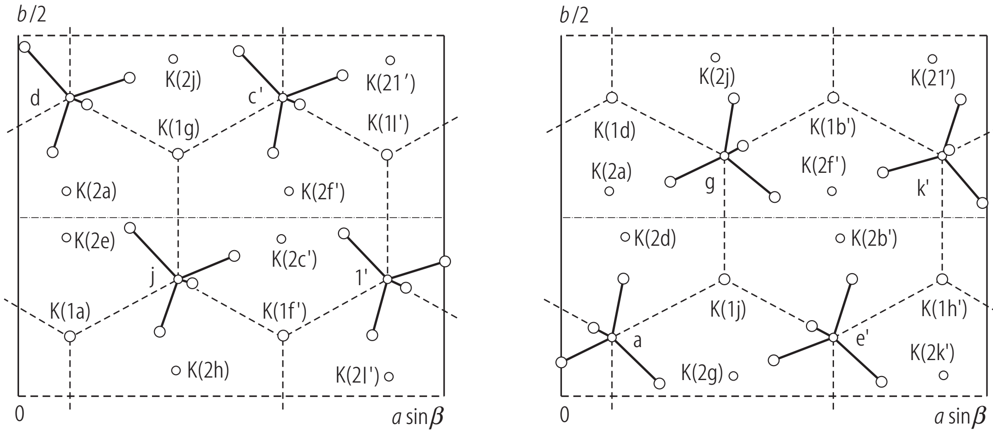

Fig. 39A-9-002. K_2ZnCl_4. Crystal structure of phase IV [93Mas]. Projection along the *c* axis. The right figure is for $0 < z < 1/6$ and the left one for $1/6 < z < 1/3$. Pseudo-hexagonal networks are indicated by broken lines. Symmetry code for primed atoms is $1/2 + x$, $1/2 - y$, $1/2 + z$. $T = 140$ K.

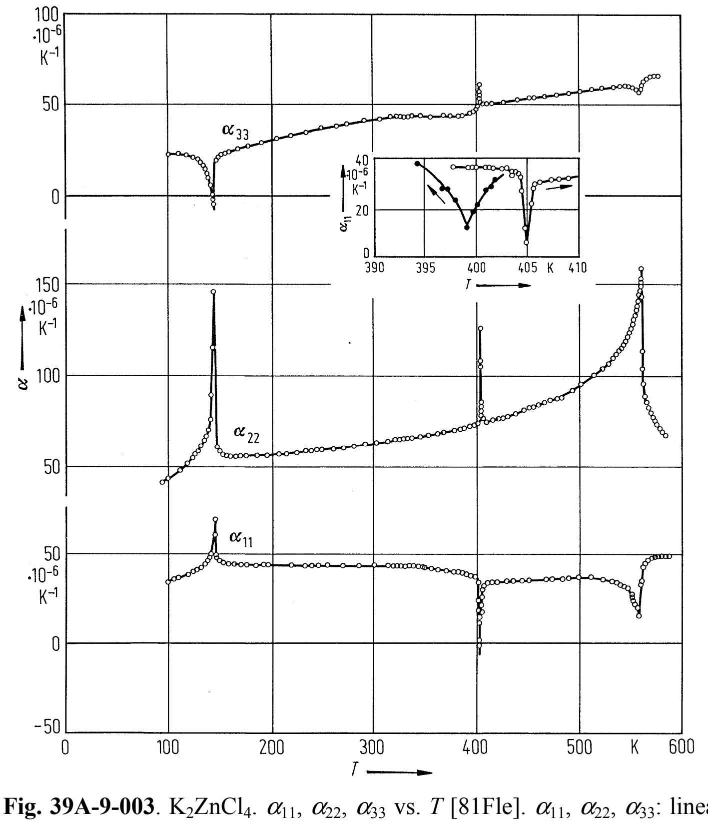

Fig. 39A-9-003. K_2ZnCl_4. α_{11}, α_{22}, α_{33} vs. *T* [81Fle]. α_{11}, α_{22}, α_{33}: linear thermal expansion coefficients along *a*, *b* and *c* axes. Insert shows α_{11} vs. *T* around Θ_{III-II} on heating and cooling.

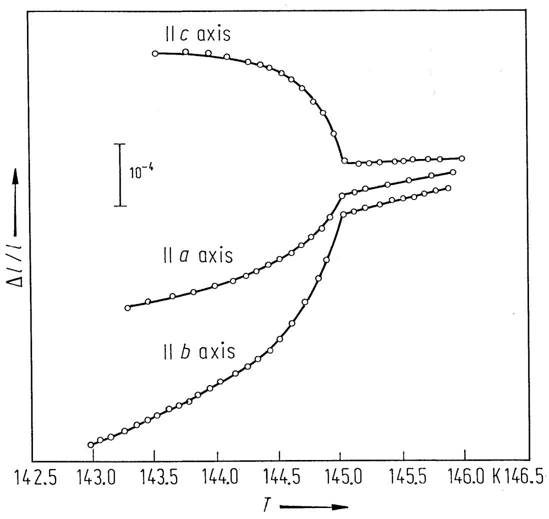

Fig. 39A-9-004. K_2ZnCl_4. $\Delta l/l$ vs. T [81Fle]. $\Delta l/l$: linear thermal expansion.

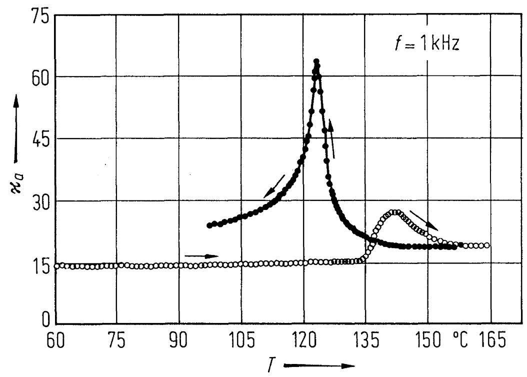

Fig. 39A-9-005. K_2ZnCl_4. κ_a vs. T [78Ges].

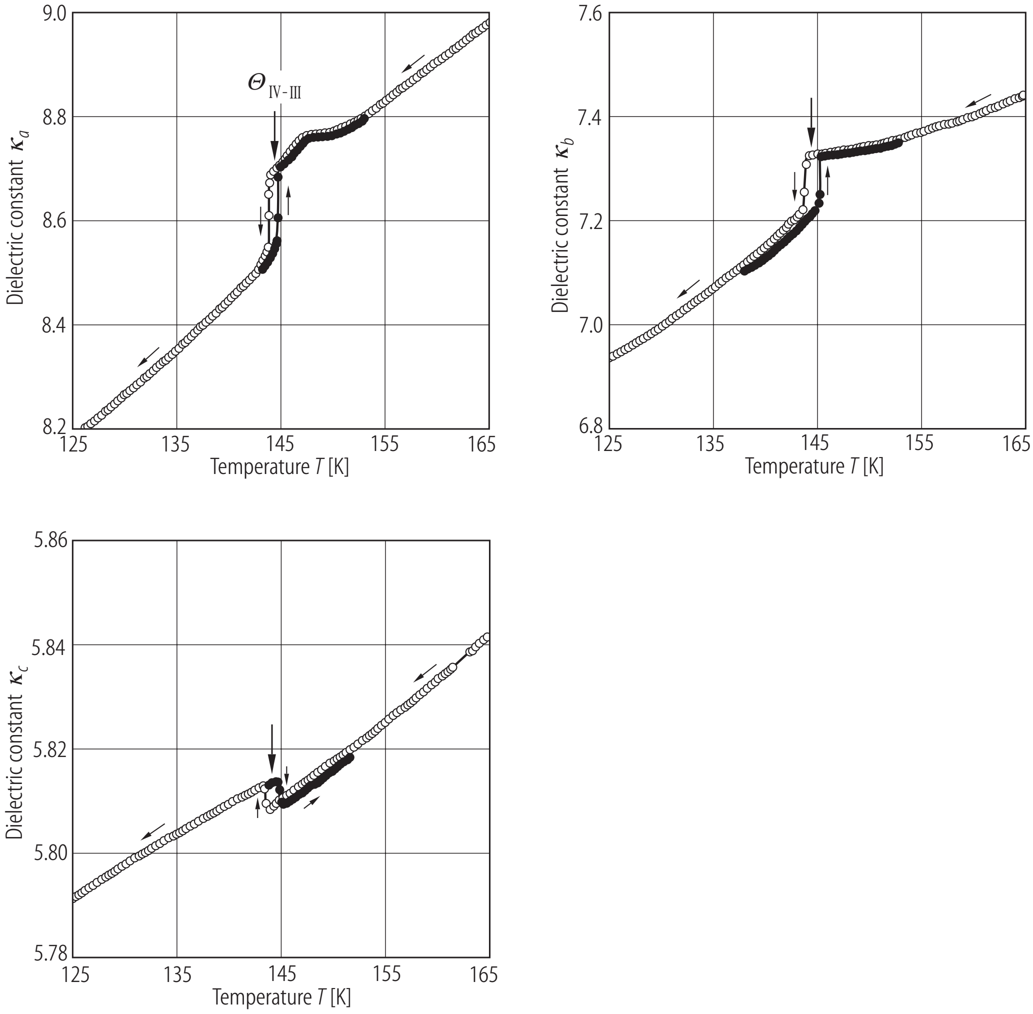

Fig. 39A-9-006. K_2ZnCl_4. κ vs. T [92Ges]. f = 100 kHz.

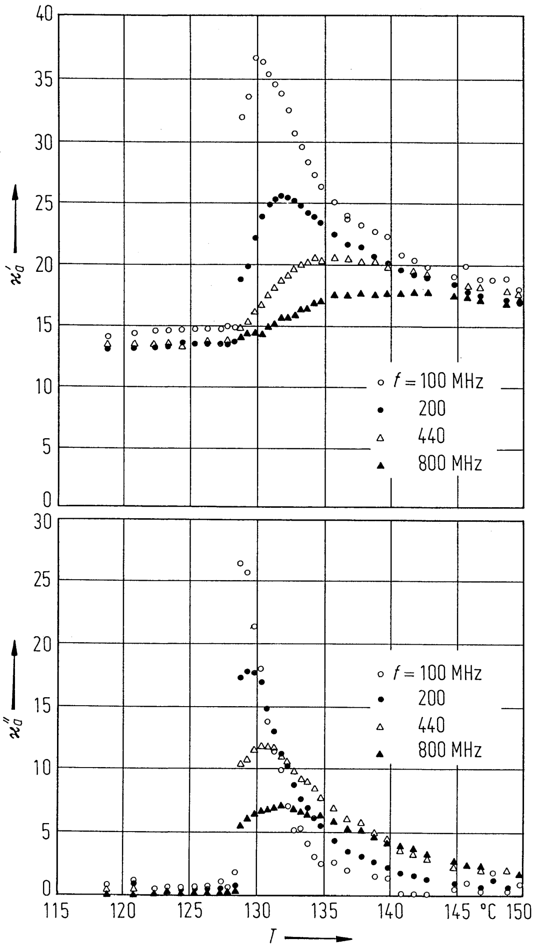

Fig. 39A-9-007. K_2ZnCl_4. κ_a', κ_a'' vs. T [84Ema]. Parameter: *f*. On heating.

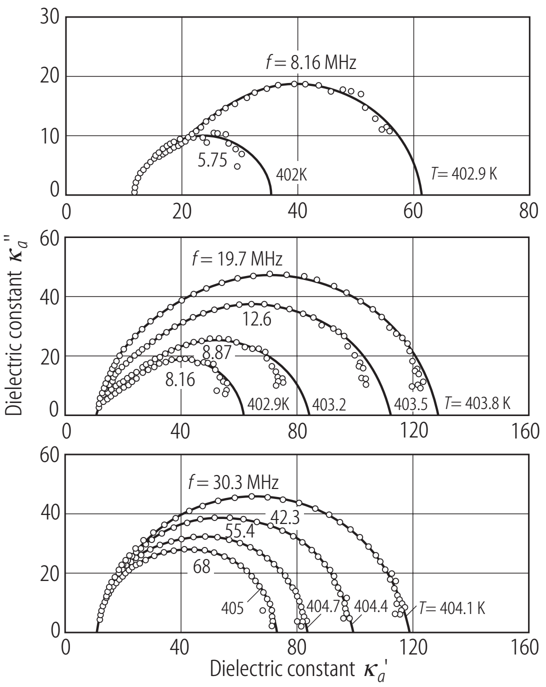

Fig. 39A-9-008. K_2ZnCl_4. Cole-Cole diagram of complex dielectric constant [92Pan].

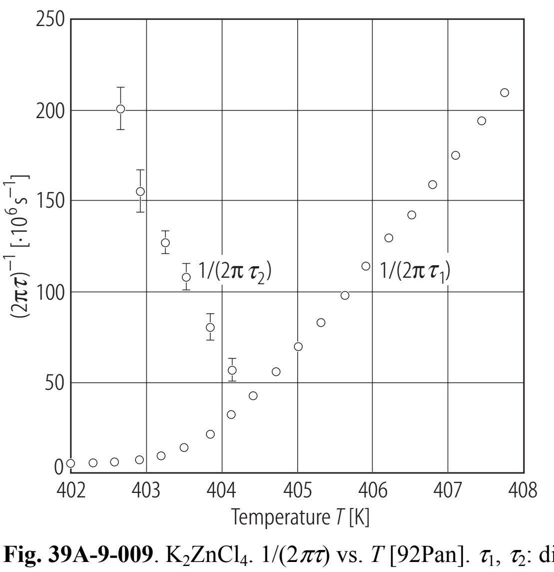

Fig. 39A-9-009. K_2ZnCl_4. $1/(2\pi\tau)$ vs. T [92Pan]. τ_1, τ_2: dielectric relaxation times of two relaxations.

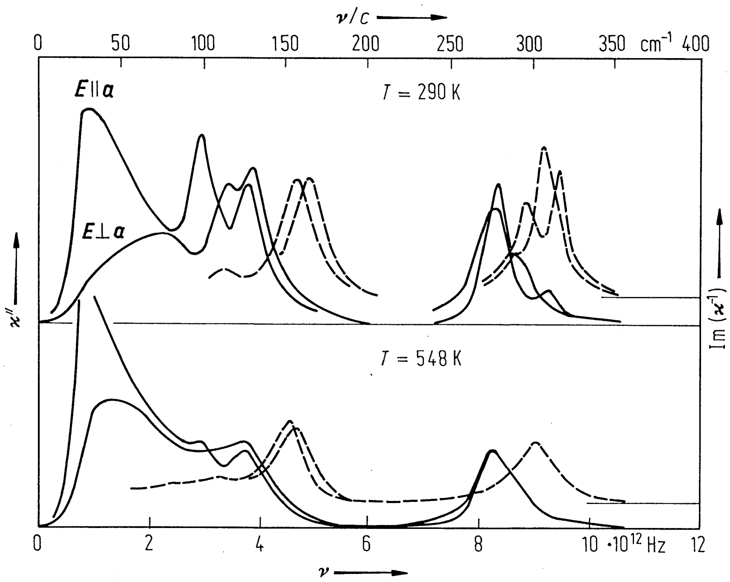

Fig. 39A-9-010. K_2ZnCl_4. κ'', Im(κ^{-1}) vs. ν [84Ech]. κ'': imaginary part of the dielectric constant obtained from the infrared reflection spectra for ***E*** ∥ ***a*** and ***E*** ⊥ ***a***. Solid curves: κ'' representing TO modes. Dashed curves: Im(κ^{-1}) representing LO modes.

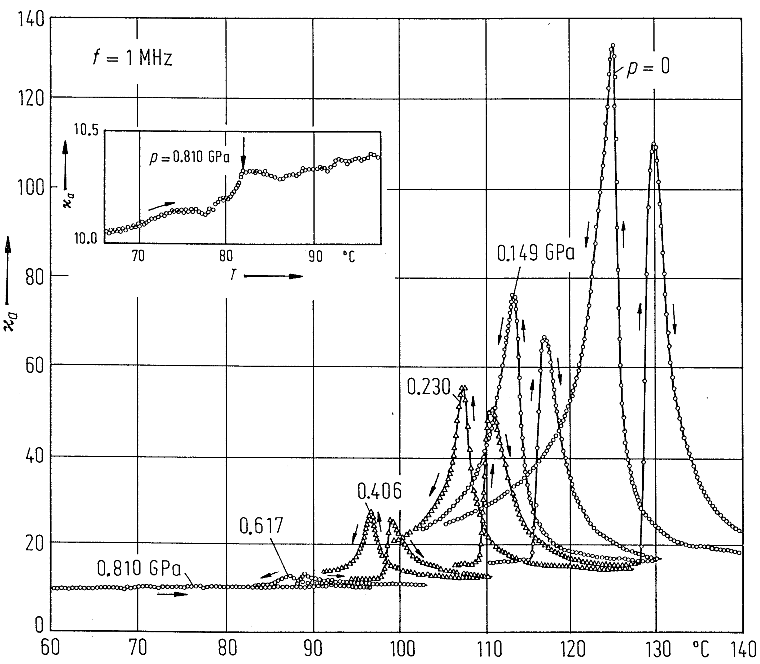

Fig. 39A-9-011. K_2ZnCl_4. κ_a vs. T [84Ges1]. Parameter: p. f = 1 MHz.

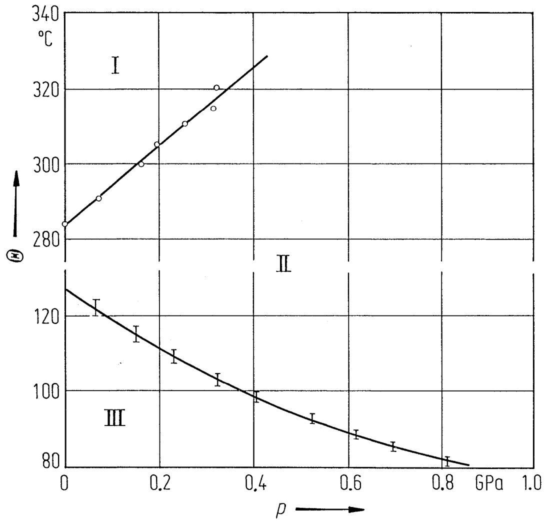

Fig. 39A-9-012. K_2ZnCl_4. Θ vs. p [84Ges1].

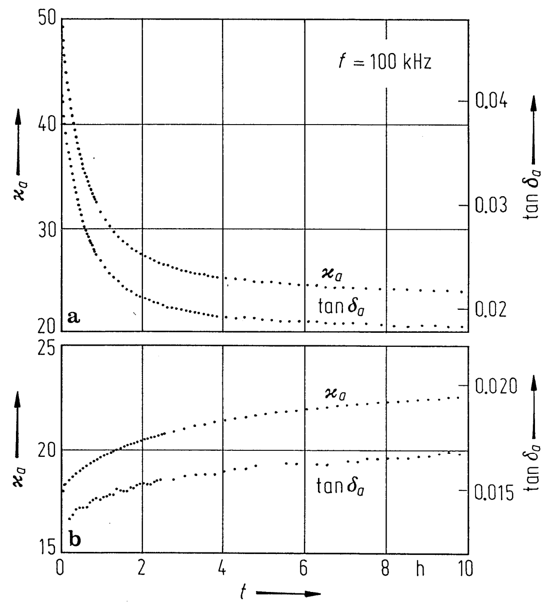

Fig. 39A-9-013. K_2ZnCl_4. κ_a, tan δ_a vs. t [87Mas]. f = 100 kHz. (**a**) The temperature was held at 406.9 K on a heating run. (**b**) The temperature was held at 406.6 K on a cooling run.

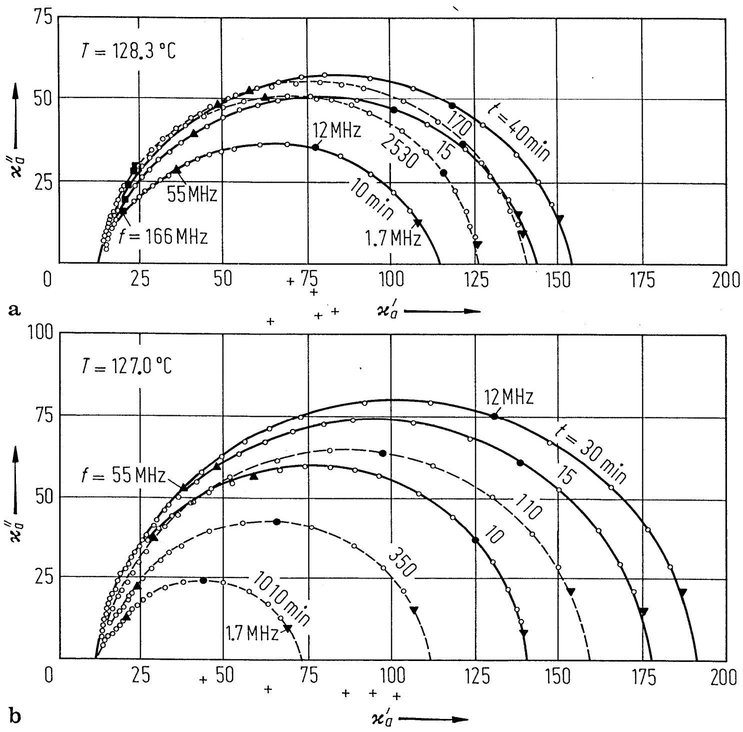

Fig. 39A-9-014. K_2ZnCl_4. Time evolution of the Cole-Cole diagram [85Ema]. Parameter: *t*. (**a**) During the III-to-II transition. Temperature was quickly raised from 127.6 °C (phase III) to 128.3 °C (phase II). (**b**) During the II-to-III transition. Temperature was quickly lowered from 127.9 °C (phase II) to 127.0 °C (phase III). Time was measured from the start of temperature increase or decrease. Plus sign: centers of the circular arcs.

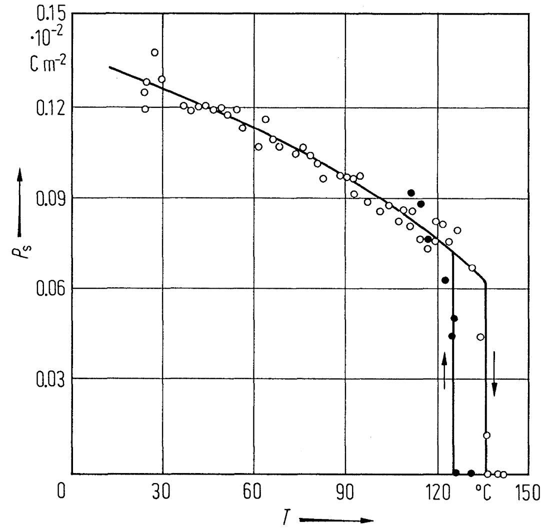

Fig. 39A-9-015. K_2ZnCl_4. P_s vs. T [78Ges].

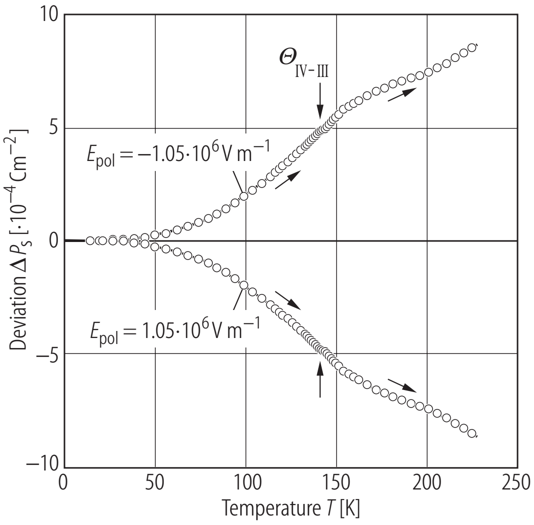

Fig. 39A-9-016. K_2ZnCl_4. ΔP_s vs. T [92Ges]. Pyroelectric charge measurement. ΔP_s: deviation of the spontaneous polarization from the value extrapolated to 0 K. E_{pol}: poling electric field.

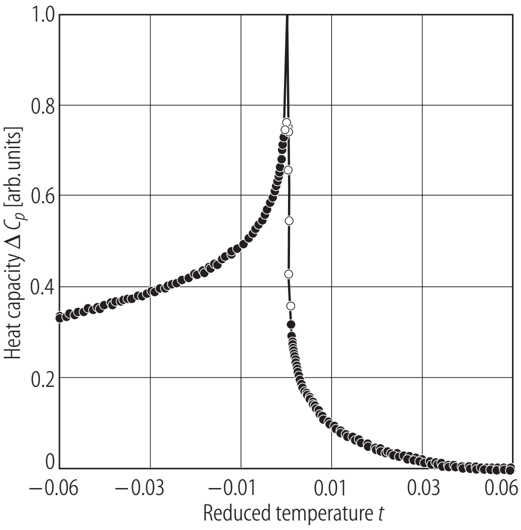

Fig. 39A-9-017. K_2ZnCl_4. ΔC_p vs. t [95Hag]. ΔC_p: excess heat capacity at constant pressure. $t = (T - \Theta_{II-I})/\Theta_{II-I}$. ac calorimetric method.

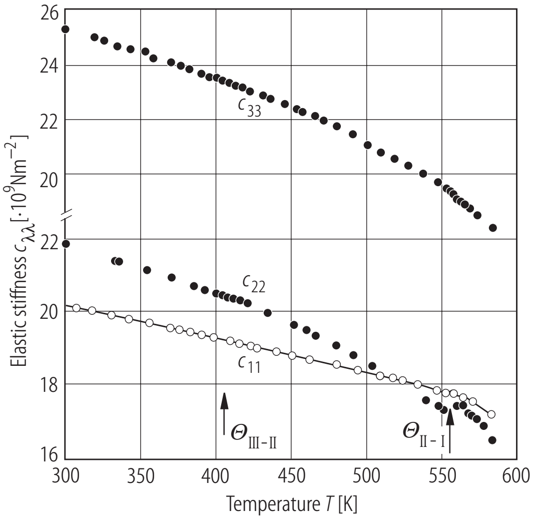

Fig. 39A-9-018. K_2ZnCl_4. $c_{\lambda\lambda}$ vs. T [88Qui]. Brillouin scattering. $\lambda = 514.5$ nm.

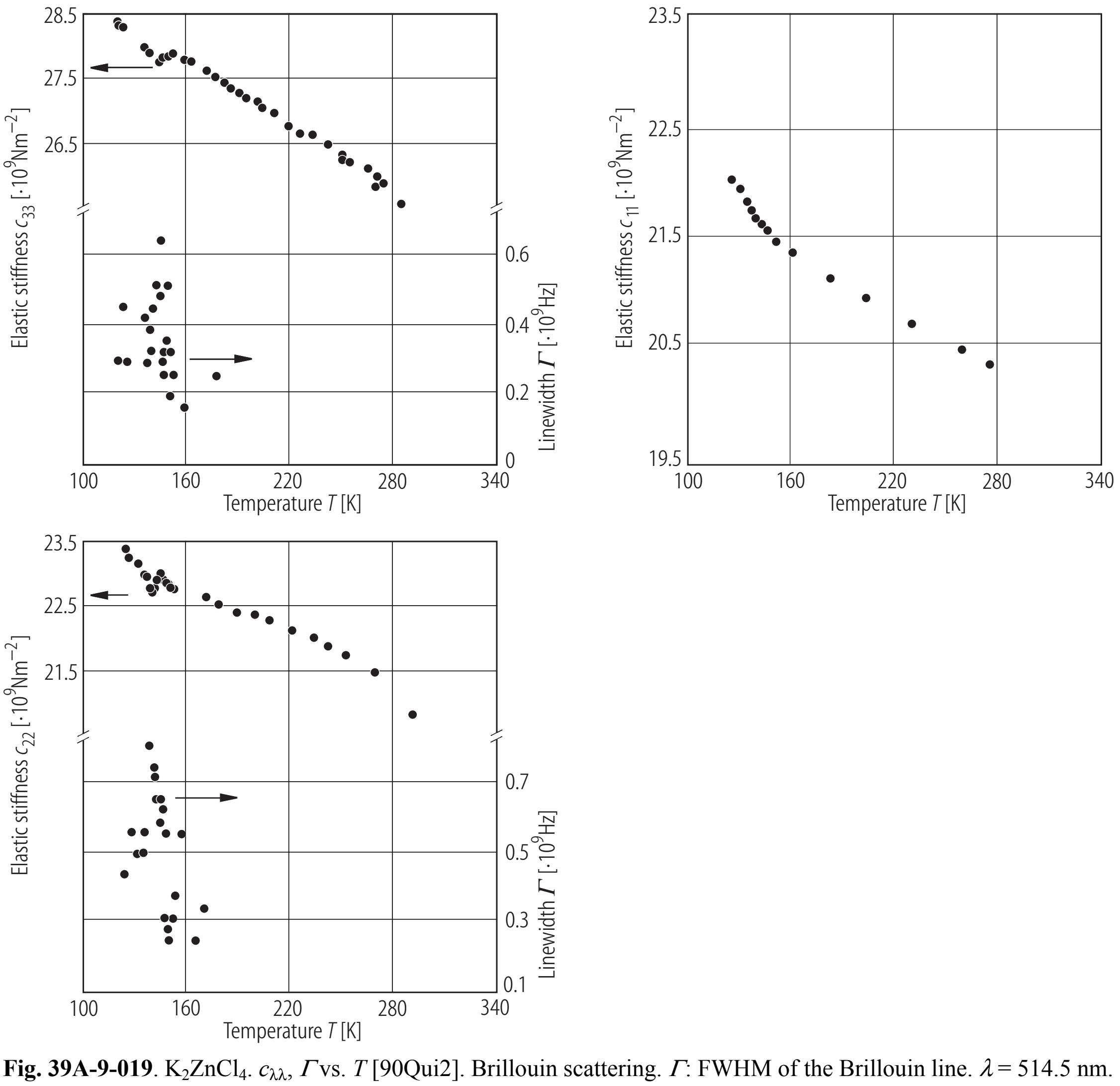

Fig. 39A-9-019. K_2ZnCl_4. $c_{\lambda\lambda}$, Γ vs. T [90Qui2]. Brillouin scattering. Γ: FWHM of the Brillouin line. $\lambda = 514.5$ nm.

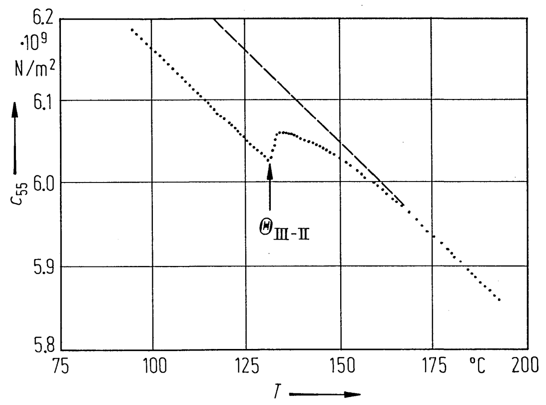

Fig. 39A-9-020. K_2ZnCl_4. c_{55} vs. T [81Hir]. Ultrasonic measurement.

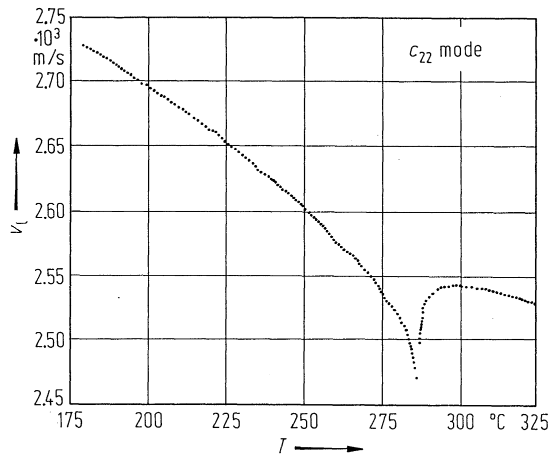

Fig. 39A-9-021. K_2ZnCl_4. v_l vs. T [80Hir]. v_l: sound velocity of c_{22} longitudinal mode. f = 10 MHz.

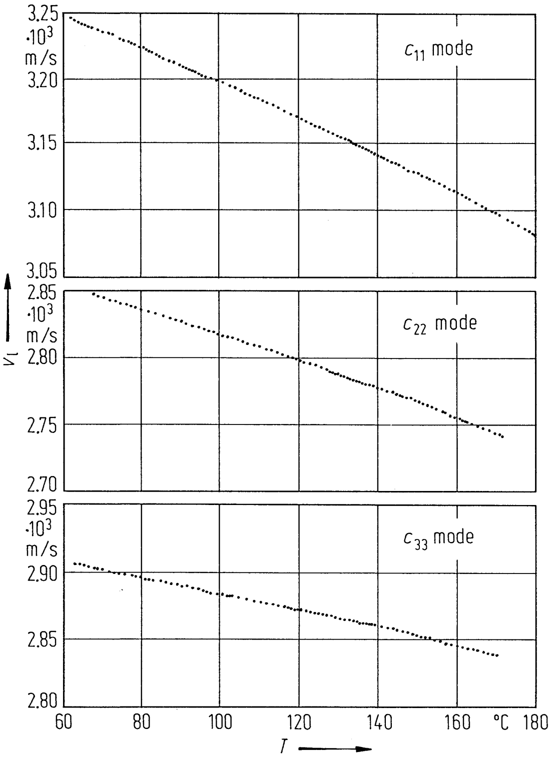

Fig. 39A-9-022. K_2ZnCl_4. v_l vs. T [80Hir]. v_l: longitudinal sound velocities. f = 10 MHz.

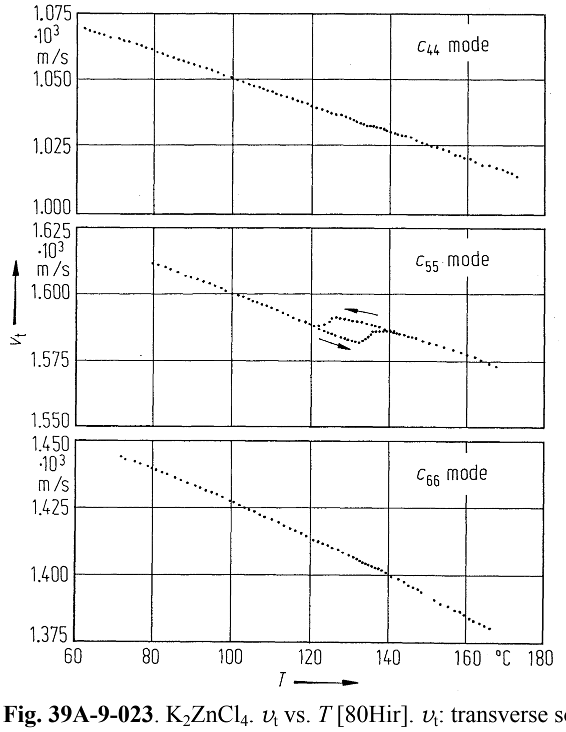

Fig. 39A-9-023. K_2ZnCl_4. v_t vs. T [80Hir]. v_t: transverse sound velocities. f = 15 MHz.

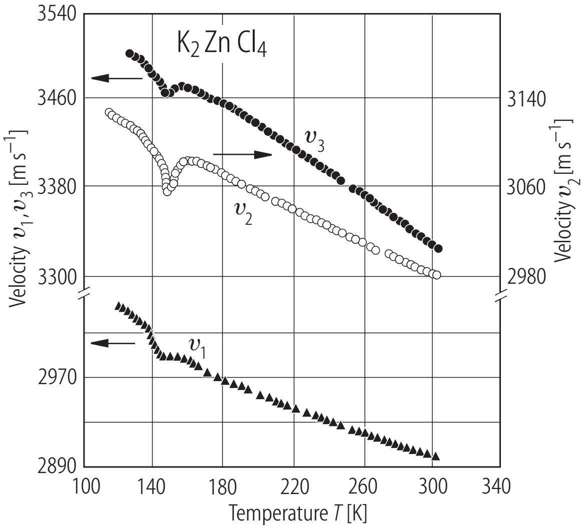

Fig. 39A-9-024. K_2ZnCl_4. υ_i vs. T [93Nas]. υ_i: longitudinal sound velocities. f = 30 MHz.

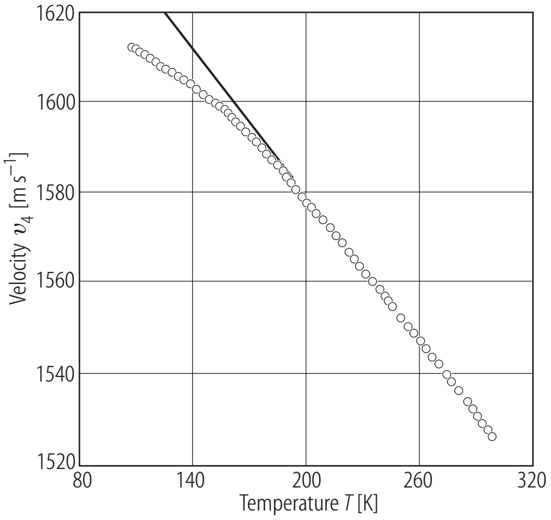

Fig. 39A-9-025. K_2ZnCl_4. υ_4 vs. T [93Nas]. υ_4: transverse sound velocity propagating along b axis and polarized along c axis. f = 30 MHz.

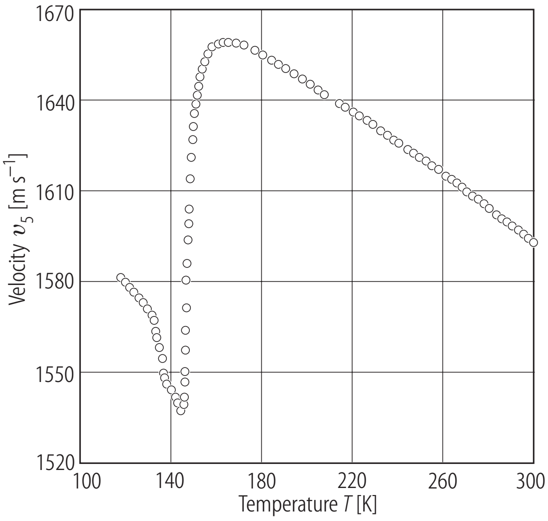

Fig. 39A-9-026. K_2ZnCl_4. v_5 vs. T [93Nas]. v_5: transverse sound velocity propagating along a axis and polarized along c axis. f = 30 MHz.

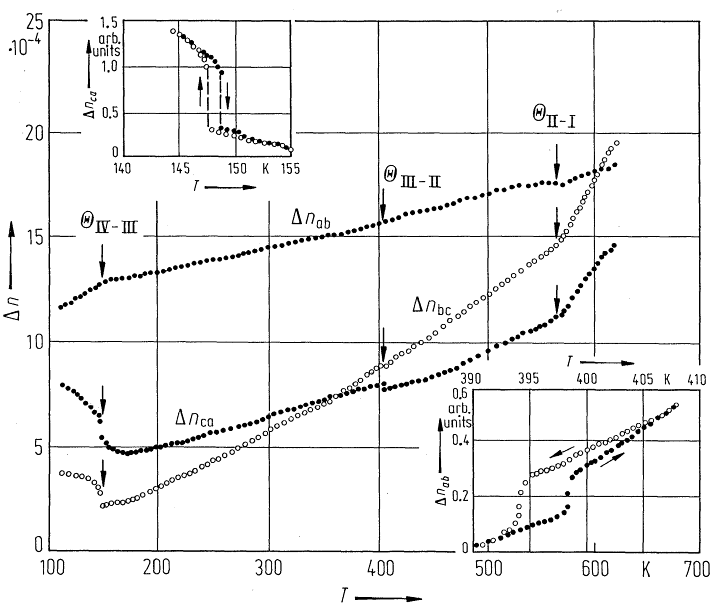

Fig. 39A-9-027. K_2ZnCl_4. Δn vs. T [85Mel]. Inserts: precise measurements around Θ_{III-II} and Θ_{IV-III}. λ = 632.8 nm.

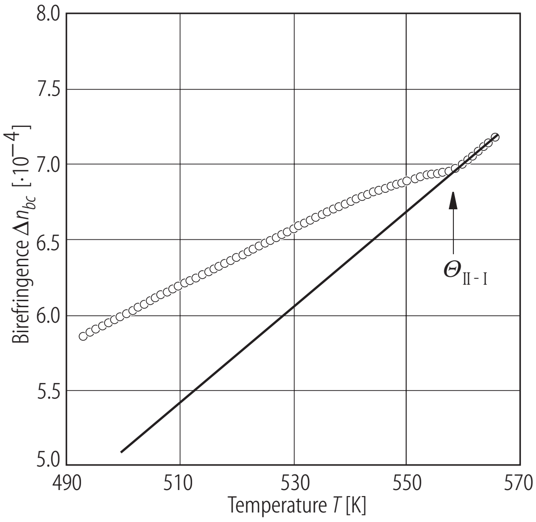

Fig. 39A-9-028. K_2ZnCl_4. Δn_{bc} vs. T [96Kim]. Δn_{bc}: birefringence along the a axis. $\lambda = 632.8$ nm.

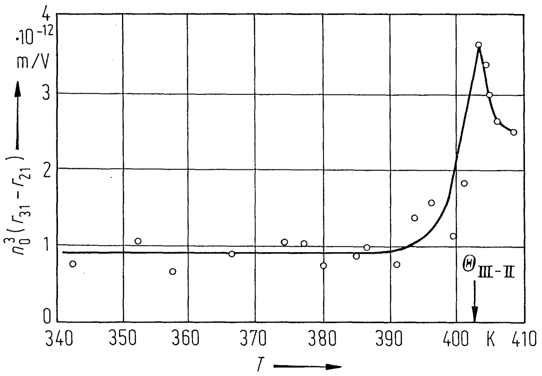

Fig. 39A-9-029. K_2ZnCl_4. $n_0^3\,(r_{31} - r_{21})$ vs. T [85Vlo]. $\lambda = 632.8$ nm.

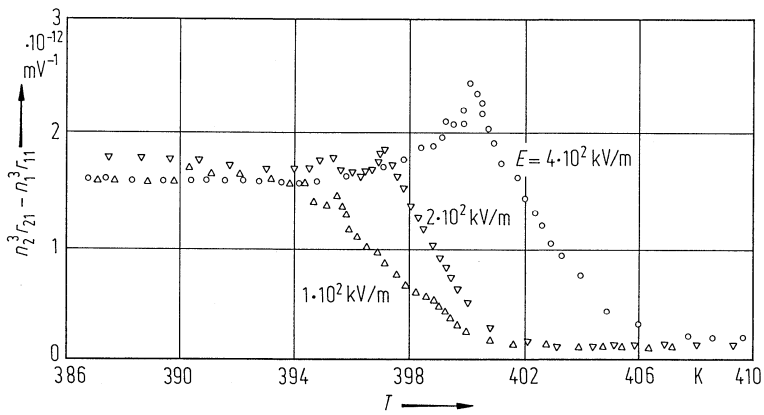

Fig. 39A-9-030. K_2ZnCl_4. $n_2^3\,r_{21} - n_1^3\,r_{11}$ vs. T [85Mel]. Parameter: E. $\lambda = 632.8$ nm.

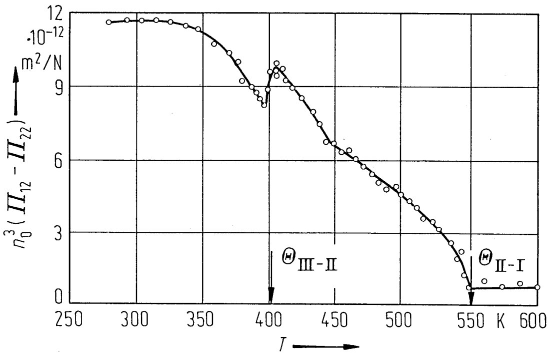

Fig. 39A-9-031. K_2ZnCl_4. $n_0^3\,(\Pi_{12}-\Pi_{22})$ vs. T [85Vlo]. $\lambda = 632.8$ nm.

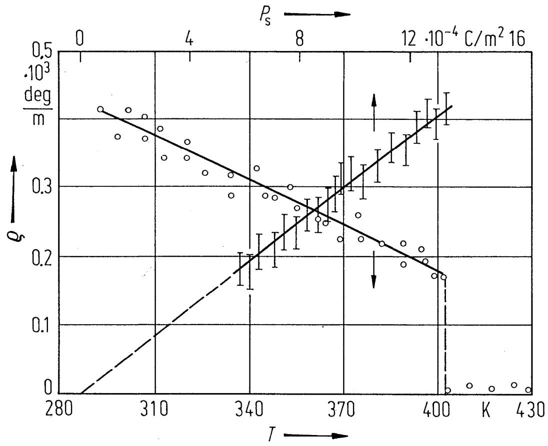

Fig. 39A-9-032. K_2ZnCl_4. ρ vs. T, P_s [85Vlo]. ρ: optical rotatory power. $\lambda = 632.8$ nm.

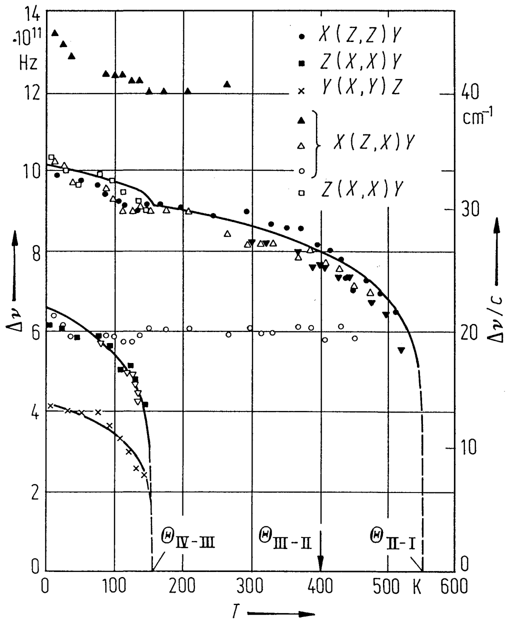

Fig. 39A-9-033. K_2ZnCl_4. $\Delta\nu$ vs. T [86Sek]. Full circle, full square and cross indicate mode frequencies obtained by fitting the Raman spectra with the spectral function. Full upside triangle, open upside triangle, open circle and open square indicate the peak positions of the Raman lines. Open downside triangle and full downside triangle are the results of [82Qui]. Scattering geometries are given in the figure.

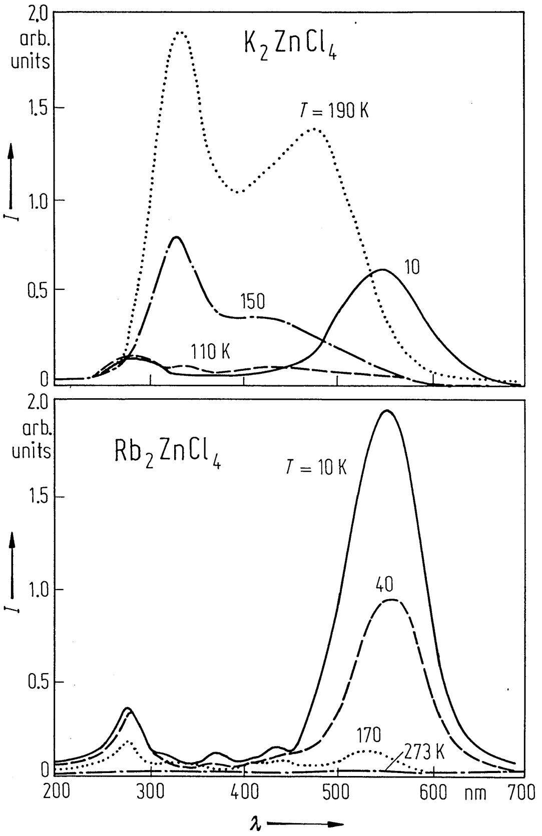

Fig. 39A-9-034. K_2ZnCl_4, Rb_2ZnCl_4. *I* vs. *λ* [86Mar]. Parameter: *T*. *I*: X-ray induced luminescent emission intensity.

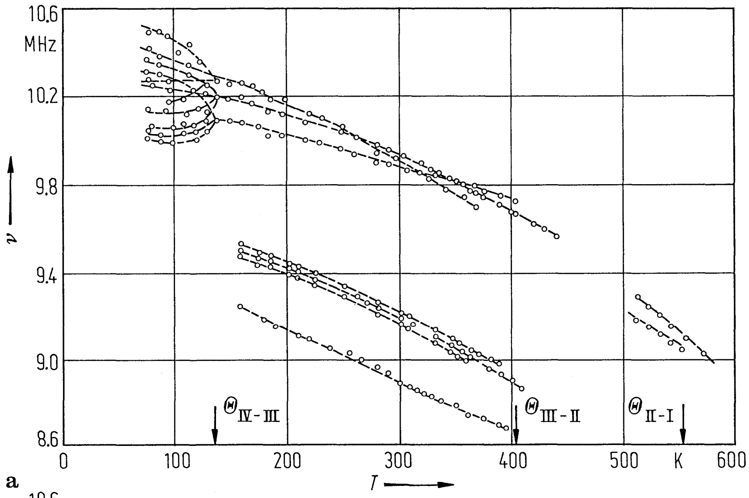

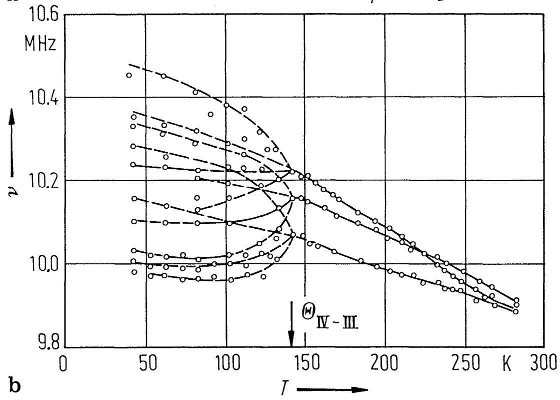

Fig. 39A-9-035. K_2ZnCl_4. ν vs. T [83Mil]. ν: ^{35}Cl NQR frequency. (**a**) All lines, (**b**) enlarged figure of the upper left corner of (**a**).

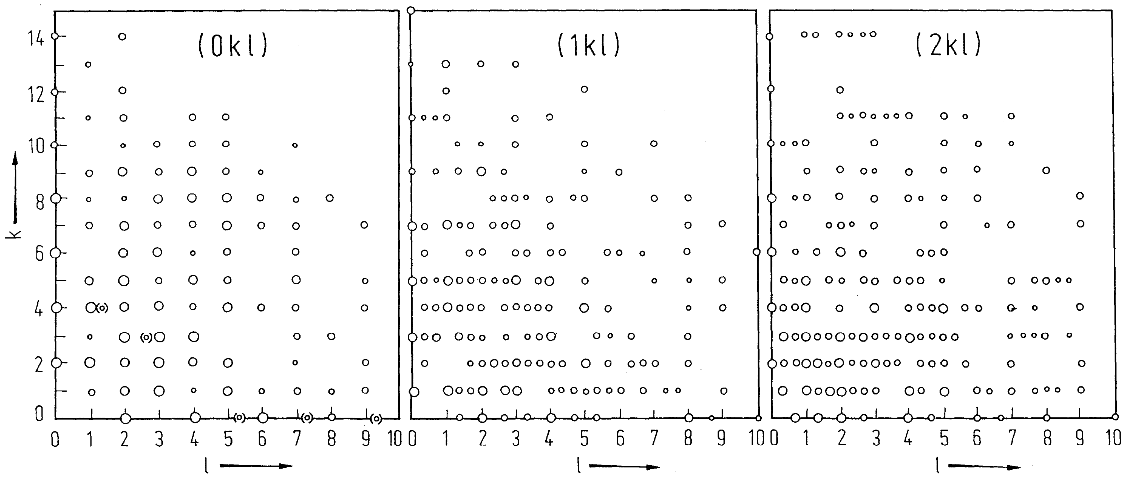

Fig. 39A-9-036. K_2ZnCl_4. Bragg intensities in (0 k l), (1 k l) and (2 k l) at RT [80Ito].

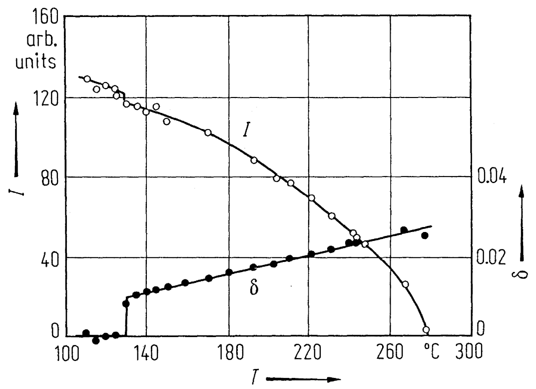

Fig. 39A-9-037. K_2ZnCl_4. *I*, δ vs. *T* [79Ges]. *I*: integrated satellite intensity at (2, 0, 2/3 + δ), δ: misfit parameter which is related to modulation wave number vector by $\boldsymbol{q} = (1/3 - \delta)\boldsymbol{c}^*$ ($\boldsymbol{c}^*$: unit cell vector in reciprocal space of phase I).

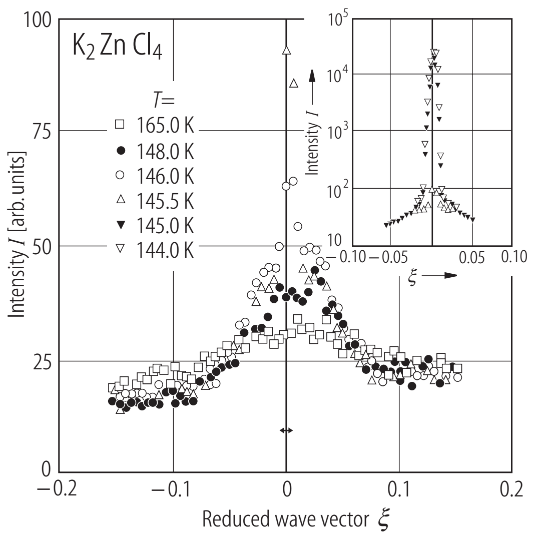

Fig. 39A-9-038. K_2ZnCl_4. *I* vs. ξ [94Has]. *I*: X-ray diffuse scattering intensity at (2.5 +ξ, 1.5, 0). Parameter: *T*. The arrow shows FWHM of the Bragg reflection (2.5, 1.5, 0) at 144.0 K. $\Theta_{\rm IV-III}$ is between 145.0 K and 145.5 K.

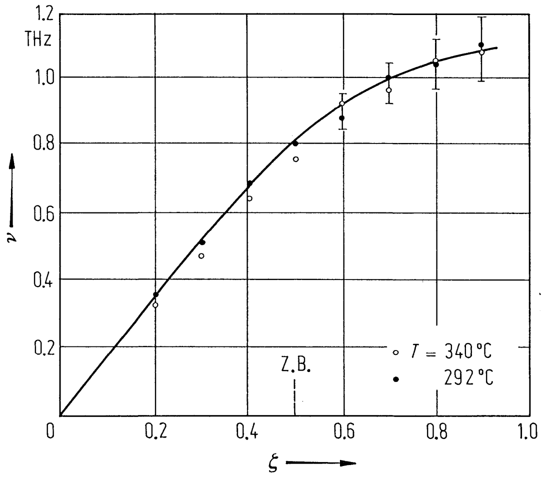

Fig. 39A-9-039. K_2ZnCl_4. ν vs. ζ [84Ges2]. Parameter: *T*. ν: frequency of transverse acoustic phonon. ζ: reduced wave vector coordinate ($\zeta = q_z/c_0$*, c_0*: reciprocal lattice constant in phase I). Z.B.: zone boundary.

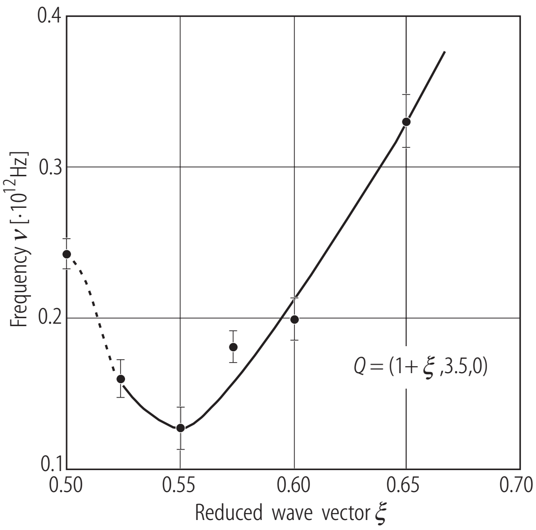

Fig. 39A-9-040. K_2ZnCl_4. Dispersion curve of the soft optic branch in the ***a**** direction [91Qui]. ν: frequency of the soft optic mode. T = 160 K. Energy scans were done with fixed incident neutron of 1.55 $Å^{-1}$.

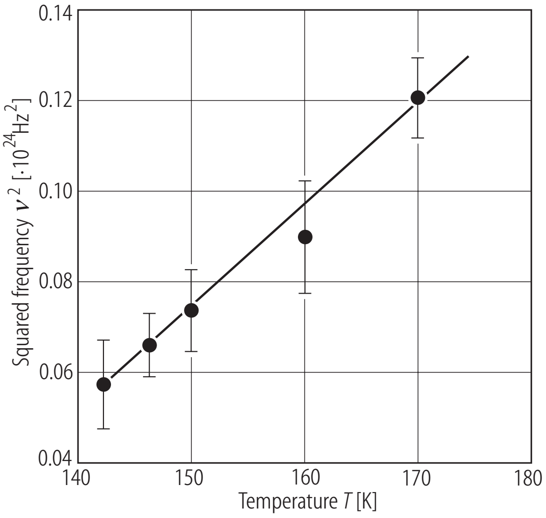

Fig. 39A-9-041. K_2ZnCl_4. ν^2 vs. T [91Qui]. ν: frequency of the soft optic mode at (***a**** + ***b****)/2 at the Brillouin zone. Energy scans were done with fixed incident neutron of 2.662 $Å^{-1}$.